DALTON
FULL PAPER

Syntheses, crystal structures and magnetic properties of two novel layered compounds: $[Fe_3(C_2O_4)_3(4,4'\text{-bpy})_4]$ and $[Co(C_2O_4)(4,4'\text{-bpy})]$ (4,4′-bpy = 4,4′-bipyridine) †

Li-Min Zheng,*[a] Xia Fang,[a] Kwang-Hwa Lii,[b] Hui-Hua Song,[a] Xin-Quan Xin,[a] Hoong-Kun Fun,[c] Kandasamy Chinnakali[c] and Ibrahim Abdul Razak[c]

[a] *State Key Laboratory of Coordination Chemistry, Coordination Chemistry Institute, Nanjing University, Nanjing 210093, China. E-mail: lmzheng@netra.nju.edu.cn; Fax: +86-25-3314502*
[b] *Institute of Chemistry, Academia Sinica, Taipei, China*
[c] *X-Ray Crystallography Unit, School of Physics, Universiti Sains Malaysia, 11800 USM, Penang, Malaysia*

Received 15th December 1998, Accepted 1st June 1999

The combination of 4,4′-bipyridine (4,4′-bpy) and oxalate ligands has resulted in the formation of two novel layered compounds $[Fe_3(C_2O_4)_3(4,4'\text{-bpy})_4]$ **1** and $[Co(C_2O_4)(4,4'\text{-bpy})]$ **2**. Both compounds exhibit two-dimensional layer structures. That of **1** consists of iron(II) oxalate chains, with the terminal and the bridging 4,4′-bpy stacking alternately between the chains. The structure of **2** contains linear chains of cobalt(II) oxalate which are cross-linked by 4,4′-bpy molecules in a perpendicular manner, leading to square grid sheets with rectangular windows. Magnetic measurements reveal that weak antiferromagnetic interactions are mediated in both compounds.

In recent years extended networks based on transition metal oxalato complexes have drawn increased attention due to their potential applications as molecular-based magnetic materials. Two- and three-dimensional frameworks bridged purely by oxalate ligand have been designed and synthesized which show tunable ferro- or antiferro-magnetic exchanges by varying the nature of the magnetic centers and charge-compensating cations.[1–9] The development of synthetic routes to novel polymeric co-ordination compounds with mixed bridging ligands, however, remains much to be explored. Success has been achieved, by combination of oxalate and 2,2′-bipyrimidine (bpym) as chelating bridging ligands, which resulted in layered compounds $[Cu_2(bpym)(C_2O_4)_2]\cdot 5H_2O$,[10] $[Mn_2(bpym)(C_2O_4)_2]\cdot 6H_2O$[11] and $[Cu_2(bpym)(C_2O_4)Cl_2]$.[12] The first two contain alternately bridging oxalate and bipyrimidine ligands, thus forming honeycombed layered structures similar to the purely oxalate bridged two-dimensional network.[2,4] The latter corrugated network consists of alternately bpym and C_2O_4 bridged copper(II) chains which are further connected through μ-chloro ligands. Such structural features could be related to the striking similarity of 2,2′-bipyrimidine and oxalate ligands in their co-ordination modes. The replacement of 2,2′-bipyrimidine by pyrazine (pyz), however, leads to the formation of $[Cu_2(C_2O_4)_2(pyz)_3]$ with a new structure type which is best described as a pleated ribbon of copper(II) oxalate linked by pyz molecules at every two copper atoms.[13]

Analogous to pyrazine, the rigid 4,4′-bipyridine (4,4′-bpy) ligand has been a useful building block for the construction of metal–organic co-ordination frameworks. A number of polymeric compounds bridged by 4,4′-bpy have been synthesized which range from the 1-D chain compound $[Co(SO_4)(H_2O)_3(4,4'\text{-bpy})]\cdot 2H_2O$,[14] 2-D square grid cationic sheets of $[Cd(4,4'\text{-bpy})(NO_3)_2]$ to 3-D interpenetrating structures of $[Ag(4,4'\text{-bpy})(NO_3)]$.[15–22] Neutral sheets have also been found in $M(4,4'\text{-bpy})X_2$ (M = Cu or Ni; X = Cl or Br),[23] where linear $\{M(4,4'\text{-bpy})\}_n$ and $\{MX_2\}_n$ chains are mutually perpendicularly arranged.

The remarkable co-ordination abilities of oxalate and 4,4′-bpy ligands have prompted us to design and synthesize new polymeric, microporous co-ordination compounds containing both ligands. The efforts resulted in the preparation of two new compounds $[Fe_3(C_2O_4)_3(4,4'\text{-bpy})_4]$ **1** and $[Co(C_2O_4)(4,4'\text{-bpy})]$ **2**, with novel layered structures. Both structures differ significantly from those with the combination of bis-chelating bridging ligands oxalate and 2,2′-bipyrimidine,[10–12] although they may be compared with that of $[Cu_2(C_2O_4)_2(pyz)_3]$.[13] In this paper the crystal structures, characterizations and magnetic properties of both compounds are reported.

Experimental

Materials and methods

All starting materials were reagent grade used as purchased. The elemental analyses were performed on a PE 240C elemental analyzer. The infrared spectra were recorded on a Fourier Nicolet FT-170SX spectrometer with pressed KBr pellets, Mössbauer spectra on an S-600 Mössbauer spectrometer using a $^{57}Co/Pd$ source. The latter spectrometer was calibrated by a standard sample of $Na_2[Fe(CN)_5(NO)]\cdot 2H_2O$ (SNP) at room temperature. The isomer shifts are reported relative to SNP. The variable temperature magnetic susceptibility data were obtained on polycrystalline samples (20.7 mg for compound **1**, 15.0 mg for **2**) from 2 to 300 K in a magnetic field of 5 kG after zero-field cooling using a SQUID magnetometer. Diamagnetic corrections were estimated from Pascal's constants.[24]

Synthesis of $[Fe_3(C_2O_4)_3(4,4'\text{-bpy})_4]$ 1

The compound was prepared as a major phase (in *ca.* 40% yield based on iron) through hydrothermal reaction of $K_3[Fe(C_2O_4)_3]\cdot 3H_2O$ (0.5 mmol, 0.2454 g), 4,4′-bipyridine (0.5 mmol, 0.0961 g) and water (10 mL) at 180 °C for 20 h. Red needles of **1** were manually picked and used for single crystal structural

† *Supplementary data available*: powder XRD pattern, IR spectra, unit-cell contents. Available from BLDSC (No. SUP 57574, 6 pp.) or the RSC Library. See Instructions for Authors, 1999, Issue 1 (http://www.rsc.org/dalton).

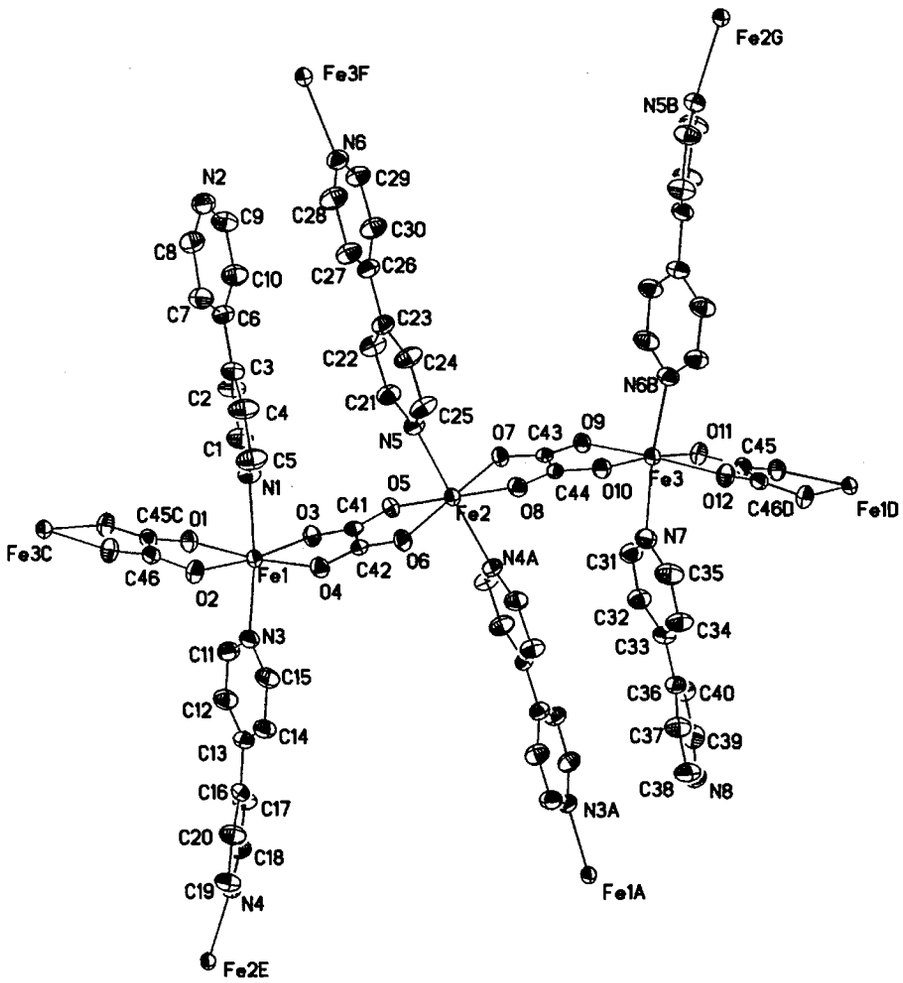

Fig. 1 The asymmetric unit of compound **1** (ellipsoids at 50% probability). The H atoms are omitted.

determination and property measurements (Found: C, 52.04; H, 3.13; N, 10.48. Calc. for $C_{46}H_{32}Fe_3N_8O_{12}$: C, 52.30; H, 3.03; N, 10.61%). IR (KBr): 3444w (br), 1668m, 1608s, 1535w, 1488w, 1412m, 1357w, 1312m, 1219w, 1078w, 1045w, 1005w, 861w, 810m, 799m, 734w, 629m, 618m, 574w and 506m cm^{-1}.

Synthesis of $[Co(C_2O_4)(4,4'\text{-bpy})]$ 2

The hydrothermal treatment of a mixture of $Co(NO_3)_2 \cdot 6H_2O$ (0.2 mmol, 0.0588 g), $H_2C_2O_4 \cdot 2H_2O$ (0.4 mmol, 0.0501 g), 4,4′-bpy (0.2 mmol, 0.0389 g) and water (10 mL) at 180 °C for 24 h resulted in orange crystals of compound **2** (in *ca.* 50% yield based on cobalt). The product is monophasic, as judged by comparison of the powder X-ray diffraction of the bulk product with the pattern simulated from the single crystal data (Found: C, 47.36; H, 2.48; N, 9.23. Calc. for $C_{12}H_8CoN_2O_4$: C, 47.54; H, 2.60; N, 9.24%). IR (KBr): 3466w (br), 3061w, 1610s, 1537w, 1493w, 1417m, 1357w, 1315m, 1223w, 1079w, 1046w, 1008w, 818m, 808m, 734w, 634m and 488m cm^{-1}. The direct reactions between the chemicals used in the hydrothermal syntheses of **1** and **2** were unsuccessful.

Crystallography

Crystals of dimensions $0.38 \times 0.1 \times 0.1$ (compound **1**) and $0.22 \times 0.20 \times 0.16$ mm (**2**) were used for indexing and intensity data collection on a Siemens Smart-CCD diffractometer equipped with a normal focus, 3 kW sealed tube X-ray source and graphite-monochromated Mo-Kα radiation ($\lambda = 0.71073$ Å) at 293 K. Empirical absorption corrections were applied for both compounds by using the SADABS program for the Siemens area detector. Lorentz-polarization and secondary extinction corrections were applied for **1**. The structures were solved by direct methods and refined by using SHELXTL.[25] All non-hydrogen atoms in both structures were refined with anisotropic displacement parameters. The hydrogen atoms in **1** were introduced in idealized positions and refined isotropically with fixed thermal parameters, those in **2** were localized from a Fourier-difference map and refined isotropically. Some relevant crystallographic data and structure determination parameters are listed in Table 1, selected bond lengths and angles in Tables 2 and 3 for **1** and **2**, respectively.

CCDC reference number 186/1483.

See http://www.rsc.org/suppdata/dt/1999/2311/ for crystallographic files in .cif format.

Results and discussion

Infrared spectra

The infrared spectra of compounds **1** and **2** (see SUP 57574) exhibit characteristic bands for both oxalate and 4,4′-bipyridine ligands. For **1** the peaks at 1668 (ν_{CO}), 1357, 1312 (ν_{CC}) and 810 cm^{-1} (δ_{OCO}) are attributed to the co-ordinated oxalate group. The peak at 506 cm^{-1} is assigned to ν_{Fe-O}, which is higher than that for $[Fe(C_2O_4)(H_2O)_2]$ (490 cm^{-1}).[26] In addition, the aromatic C–C and C–N stretching vibration absorptions appear at 1608, 1535, 1488 and 1412 cm^{-1}. The bands in the region 618–1219 cm^{-1} can be assigned to the CH in-plane or out-of-plane bend, ring breathing and ring deformation absorptions of 4,4′-bipyridine.[27] As the band at 618 cm^{-1} of the free ligand is very sensitive and shifts to a higher frequency after co-ordination to a metal ion,[27] the appearance of two peaks at 629 and 618 cm^{-1} suggests the presence of two kinds of 4,4′-bpy which is consistent with the single crystal structural analysis. The infrared spectrum of **2** is similar to that of **1** except that only one peak (634 cm^{-1}) appears near 618 cm^{-1}, which indi-

Table 1 Crystal data and structure refinement for compounds **1** and **2**

	1	**2**
Empirical formula	$C_{46}H_{32}Fe_3N_8O_{12}$	$C_{12}H_8CoN_2O_4$
Formula weight	1056.35	303.13
Crystal system	Monoclinic	Orthorhombic
Space group	$P2_1/c$	$Imm2$
a/Å	16.2475(2)	10.9768(3)
b/Å	15.9840(2)	11.4017(3)
c/Å	16.3856(1)	5.4032(1)
β/°	94.2776(3)	
U/Å^3	4243.49(8)	676.23(3)
Z	4	2
D_c/g cm^{-3}	1.653	1.489
μ(Mo-Kα)/cm^{-1}	10.90	12.78
F(000)	2152	306
Reflections collected	24362	2230
Independent reflections	9195 [R(int) = 0.0621]	628 [R(int) = 0.0241]
Data, restraints, parameters	9195, 0, 623	628, 1, 55
Goodness of fit of F^2	1.023	1.119
$R1$, $wR2$ [$I > 2\sigma(I)$]	0.0493, 0.0887	0.0257, 0.0666
(all data)	0.1113, 0.1127	0.0267, 0.0671
Extinction coefficient	0.00022(5)	
Absolute structure parameter		0.08(6)
$(\Delta\rho)_{max}$, $(\Delta\rho)_{min}$/e Å^{-3}	0.357, −0.541	0.302, −0.238

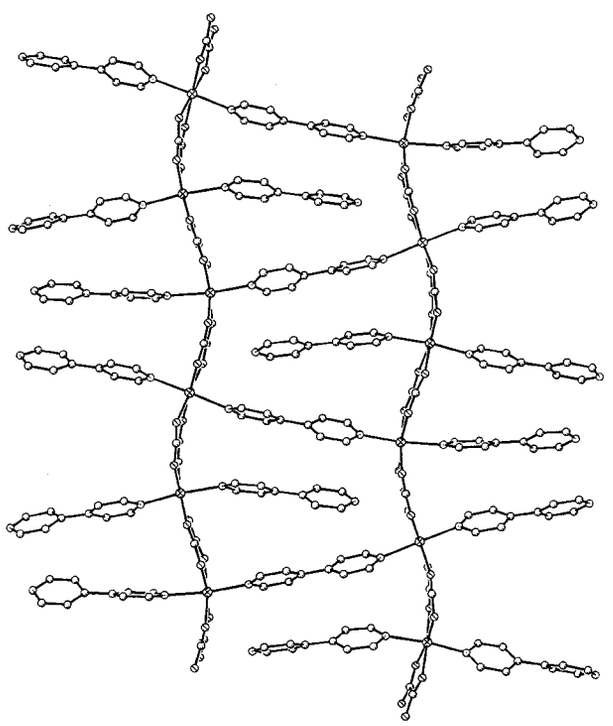

Fig. 2 One layer of compound **1** viewed along the [101] direction. The hydrogen atoms are omitted for clarity.

cates the existence of only one type of 4,4′-bpy. The band at 488 cm^{-1} is assigned to $\nu_{Co\text{-}O}$.

Structure of compound 1

The structure of compound **1** is made up of asymmetric units of $Fe_3(\mu\text{-}C_2O_4)_3(\mu\text{-}4,4'\text{-bpy})_2(4,4'\text{-bpy})_2$ with 69 non-hydrogen independent atoms (Fig. 1). Three iron centers are crystallographically distinguishable; each co-ordinates to four oxygen atoms from the oxalate anions and two nitrogen atoms from the 4,4′-bpy molecules to form a distorted octahedral environment. The oxalate anion behaves as a bridging ligand and links the three iron centers repeatedly to form infinite chains running parallel to the b axis, with zigzag undulation in the (101) plane (Fig. 2). The Fe–O distances [2.102(2)–2.126(2) Å] are comparable to those in $[Fe(bipy)_3][Fe_2(C_2O_4)_3]$ [2.122(2), 2.128(2) Å][3] and $[Fe(C_2O_4)(2,2'\text{-bpy})]$ (2,2′-bpy = 2,2′-bipyridine) [2.092(3)–2.162(4) Å].[28] The 4,4′-bpy molecule serves as either a terminal or bridging ligand. The apical positions of the Fe1 (or Fe3) octahedron are occupied by N atoms from both terminal and bridging 4,4′-bpy. The apical positions of the Fe2 octahedron, however, are filled by the N atoms from two bridging 4,4′-bpy. The Fe–N bond lengths [2.193(3)–2.290(3) Å] agree well with that in $[Fe(SCN)_2(H_2O)_2(4,4'\text{-bpy})_2]$ [2.214(2) Å],[29] although the Fe–N lengths with terminal 4,4′-bpy [2.290(3) and 2.249(3) Å for Fe1–N1 and Fe3–N7, respectively] are slightly

Table 2 Selected bond lengths (Å) and angles (°) for compound **1**

Fe(1)–O(1)	2.124(3)	Fe(1)–O(4)	2.102(2)
Fe(1)–O(2)	2.112(3)	Fe(1)–O(3)	2.106(2)
Fe(1)–N(1)	2.290(3)	Fe(1)–N(3)	2.217(3)
Fe(2)–O(5)	2.114(2)	Fe(2)–O(6)	2.119(2)
Fe(2)–O(7)	2.123(2)	Fe(2)–O(8)	2.117(2)
Fe(2)–N(4A)	2.256(3)	Fe(2)–N(5)	2.240(3)
Fe(3)–O(9)	2.104(2)	Fe(3)–O(10)	2.115(2)
Fe(3)–O(11)	2.123(2)	Fe(3)–O(12)	2.126(2)
Fe(3)–N(6B)	2.193(3)	Fe(3)–N(7)	2.249(3)
O(1)–C(45C)	1.264(4)	O(2)–C(46)	1.256(4)
O(3)–C(41)	1.259(4)	O(4)–C(42)	1.261(4)
O(5)–C(41)	1.254(4)	O(6)–C(42)	1.258(4)
O(7)–C(43)	1.250(4)	O(8)–C(44)	1.257(4)
O(9)–C(43)	1.260(4)	O(10)–C(44)	1.267(4)
O(11)–C(45)	1.246(4)	O(12)–C(46D)	1.249(4)
C(41)–C(42)	1.556(5)	C(43)–C(44)	1.547(5)
C(45)–C(46D)	1.559(5)		
O(4)–Fe(1)–O(3)	79.58(9)	O(4)–Fe(1)–O(2)	98.91(9)
O(3)–Fe(1)–O(2)	171.99(9)	O(3)–Fe(1)–O(1)	101.40(9)
O(4)–Fe(1)–O(1)	172.84(9)	O(2)–Fe(1)–O(1)	79.12(9)
O(4)–Fe(1)–N(3)	97.61(10)	O(3)–Fe(1)–N(3)	98.29(10)
O(2)–Fe(1)–N(3)	89.71(10)	O(1)–Fe(1)–N(3)	89.28(10)
O(4)–Fe(1)–N(1)	87.29(10)	O(3)–Fe(1)–N(1)	87.31(10)
O(2)–Fe(1)–N(1)	84.75(10)	O(1)–Fe(1)–N(1)	85.68(10)
N(3)–Fe(1)–N(1)	173.13(12)	O(5)–Fe(2)–O(8)	178.78(9)
O(5)–Fe(2)–O(6)	79.69(9)	O(8)–Fe(2)–O(6)	100.98(9)
O(5)–Fe(2)–O(7)	99.66(9)	O(8)–Fe(2)–O(7)	79.65(9)
O(6)–Fe(2)–O(7)	179.05(9)	O(5)–Fe(2)–N(5)	88.87(10)
O(8)–Fe(2)–N(5)	92.15(10)	O(6)–Fe(2)–N(5)	88.56(10)
O(7)–Fe(2)–N(5)	92.13(10)	O(5)–Fe(2)–N(4A)	92.34(10)
O(8)–Fe(2)–N(4A)	86.62(10)	O(6)–Fe(2)–N(4A)	92.63(10)
O(7)–Fe(2)–N(4A)	86.69(10)	N(5)–Fe(2)–N(4A)	178.43(11)
O(9)–Fe(3)–O(10)	79.47(9)	O(9)–Fe(3)–O(11)	99.67(9)
O(10)–Fe(3)–O(11)	173.10(9)	O(9)–Fe(3)–O(12)	176.17(9)
O(10)–Fe(3)–O(12)	101.32(10)	O(11)–Fe(3)–O(12)	79.09(9)
O(9)–Fe(3)–N(6B)	94.71(10)	O(10)–Fe(3)–N(6B)	96.77(10)
O(11)–Fe(3)–N(6B)	90.12(10)	O(12)–Fe(3)–N(6B)	88.93(10)
O(9)–Fe(3)–N(7)	90.41(10)	O(10)–Fe(3)–N(7)	88.19(10)
O(11)–Fe(3)–N(7)	84.97(10)	O(12)–Fe(3)–N(7)	85.87(11)
N(6B)–Fe(3)–N(7)	173.44(12)	C(45C)–O(1)–Fe(1)	112.6(2)
C(46)–O(2)–Fe(1)	113.0(2)	C(41)–O(3)–Fe(1)	112.3(2)
C(42)–O(4)–Fe(1)	112.4(2)	C(5)–N(1)–Fe(1)	122.9(3)
C(1)–N(1)–Fe(1)	120.7(2)	C(11)–N(3)–Fe(1)	122.9(2)
C(15)–N(3)–Fe(1)	120.6(2)	C(41)–O(5)–Fe(2)	112.7(2)
C(42)–O(6)–Fe(2)	112.3(2)	C(43)–O(7)–Fe(2)	111.2(2)
C(44)–O(8)–Fe(2)	111.3(2)	C(21)–N(5)–Fe(2)	123.2(2)
C(25)–N(5)–Fe(2)	119.8(2)	C(19)–N(4)–Fe(2E)	120.7(2)
C(18)–N(4)–Fe(2E)	121.8(2)	C(43)–O(9)–Fe(3)	112.8(2)
C(44)–O(10)–Fe(3)	111.8(2)	C(45)–O(11)–Fe(3)	113.0(2)
C(46D)–O(12)–Fe(3)	112.8(2)	C(29)–N(6)–Fe(3F)	122.5(2)
C(28)–N(6)–Fe(3F)	121.0(2)	C(31)–N(7)–Fe(3)	121.7(3)
C(35)–N(7)–Fe(3)	119.8(2)	O(5)–C(41)–O(3)	125.9(3)
O(5)–C(41)–C(42)	117.4(3)	O(3)–C(41)–C(42)	116.7(3)
O(6)–C(42)–O(4)	125.5(3)	O(6)–C(42)–C(41)	117.5(3)
O(4)–C(42)–C(41)	117.0(3)	O(7)–C(43)–O(9)	125.4(3)
O(7)–C(43)–C(44)	117.6(3)	O(9)–C(43)–C(44)	117.0(3)
O(8)–C(44)–O(10)	124.9(3)	O(8)–C(44)–C(43)	117.9(3)
O(10)–C(44)–C(43)	117.1(3)	O(11)–C(45)–O(1D)	125.7(3)
O(11)–C(45)–C(46D)	117.5(3)	O(1D)–C(45)–C(46D)	116.8(3)
O(12C)–C(46)–O(2)	125.9(3)	O(12C)–C(46)–C(45C)	117.2(3)
O(2)–C(46)–C(45C)	116.9(3)		

Symmetry transformations used to generate equivalent atoms: A $-x+1, y+\frac{1}{2}, -z+\frac{1}{2}$; B $-x, y+\frac{1}{2}, -z+\frac{3}{2}$; C $x, y-1, z$; D $x, y+1, z$; E $-x+1, y-\frac{1}{2}, -z+\frac{1}{2}$; F $-x, y-\frac{1}{2}, -z+\frac{3}{2}$.

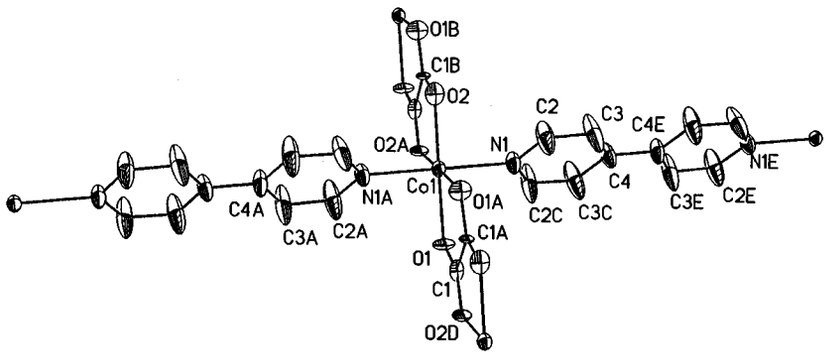

Fig. 3 The co-ordination around the Co in compound **2** (ellipsoids at 50% probability). The H atoms are omitted.

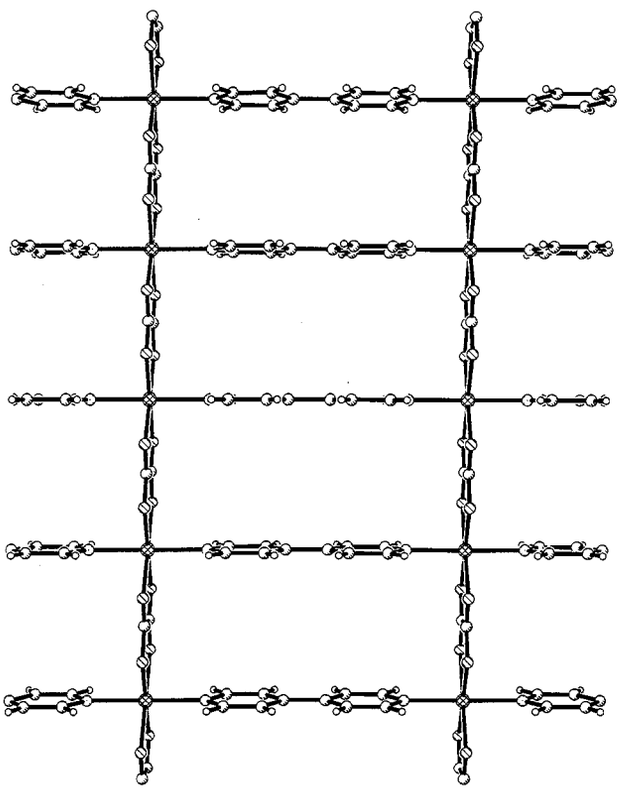

Fig. 4 One layer of compound **2** viewed along the [100] direction.

longer. Consequently, condensed two-dimensional sheets are constructed in the (101) planes (Fig. 2), with the terminal and the bridging 4,4′-bpy stacking alternately between the iron(II) oxalate chains. The bridging 4,4′-bpy molecules connect the Fe2 atom with both Fe1 and Fe3 atoms to form iron "trimers" in the layer. The two pyridine rings of each 4,4′-bpy are twisted with dihedral angles of 28.4–38.9°. The intra-layer Fe···Fe separations are 5.397–5.431 Å through the oxalate bridges and 11.494–11.543 Å through the 4,4′-bpy bridges, respectively. The interlayer distance is 5.55 Å. Weak hydrogen bondings are observed within the layer and between the layers. The four shortest C···O distances are 3.030(5), 3.164(5), 3.166(5) and 3.193(5) Å for C35···O12, C29···O12^{i}, C11···O1 and C1···O1 (symmetry code: i $-x$, $y-\frac{1}{2}$, $-z+\frac{3}{2}$), respectively.

The structure of compound **1** is unique compared with that of $[Cu_2(C_2O_4)_2(pyz)_3]$.[13] The latter contains two types of copper atoms with O_4N_2 co-ordination environments. One has only terminally co-ordinated pyz molecules while the other is linked by bridging pyz molecules.

Structure of compound 2

The structure of compound **2** is highly symmetric. Fig. 3 shows the co-ordination around the Co which exhibits an elongated octahedral environment. The basal plane consists of four oxygen atoms from two equivalent oxalate anions, whereas the apical positions are occupied by two nitrogen atoms from the symmetrically equivalent 4,4′-bpy molecules. The Co1–O bond length [mean 2.084(6) Å] can be compared with those in $[Co(bpy)_3][Co_2(C_2O_4)_3]ClO_4$ [2.070(5), 2.081(5) Å][9] and $[CoCr_2(bipy)_2(\mu\text{-}C_2O_4)_2(C_2O_4)_2(H_2O)_2]\cdot H_2O$ [2.089(6), 2.155(6) Å].[30] The Co–N distance [Co1–N 2.153(2) Å] is consistent with those in $[Co_2(4,4'\text{-bpy})_3(NO_3)_4]\cdot 4H_2O$ [2.13(1) Å].[16] Both the oxalate anion and 4,4′-bpy act as bridging ligands. The cobalt–oxalate chains along the [001] direction are linear, which is different from those in compound **1**. The adjacent chains are cross-linked by 4,4′-bpy molecules in a perpendicular manner, leading to square grid sheets in the *bc* planes with rectangular windows (Fig. 4). The two pyridine rings of 4,4′-bpy are coplanar and symmetrically related to each other. The intra-layer Co···Co separations are 5.403 Å through the oxalate bridge and 11.402 Å through the 4,4′-bpy bridge, respectively. In the crystal, the sheets are stacked along the [100] direction to give extended one-dimensional channel networks. The interlayer distance is 5.50 Å for **2**. Weak hydrogen bonding has been found within the layer and between the layers. The three shortest C···O distances are 3.260, 3.283 and 3.283 Å for C2···O2, C2···O1^{i} and C2···O1^{ii} (symmetry codes: i $-x+1$, $-y$, z; ii $-x+1$, y, z), respectively.

Clearly, the structure of compound **2** is quite different from that of **1**. This reflects, on the one hand, the co-ordination flexibilities of 4,4′-bpy either as a terminal or bridging ligand with the two pyridine rings twisted or coplanar. On the other hand, the formation of zigzag iron(II) oxalate chains in **1** may originate from the starting materials, wherein a tris-chelated iron compound was employed. It is worth noting that the oxidation state of the iron in **1** is +2, though the starting material is an iron(III) compound. A similar phenomenon has been observed in the hydrothermal synthesis of $[Fe_2(C_2O_4)(OH)_2]$.[31]

Mössbauer spectrum of compound 1

The room-temperature Mössbauer spectrum of compound **1** is shown in Fig. 5. It can be least-squares fitted with one doublet instead of three doublets corresponding to the three types of iron components observed in the crystal structure. The parameters obtained are δ (isomer shift) = 0.95 mm s^{-1}, ΔE_Q (quadrupole splitting) = 2.22 mm s^{-1}. The spectrum is typical of high-spin Fe^{II}[5,26] which is consistent with the magnetic susceptibility data of **1**.

Magnetic properties of compound 1

Fig. 6(a) shows the magnetic behavior of a powdered sample of compound **1** in the form of a χ_m *vs.* T plot where χ_m is the molar magnetic susceptibility. At 300 K the effective magnetic moment (μ_{eff}) per Fe, calculated from $\mu_{eff} = 2.828(\chi_m T)^{1/2}$, is 5.68 μ_B which is greater than the spin-only value of 4.90 μ_B for $S = 2$.

Table 3 Selected bond lengths (Å) and angles (°) for compound **2**

Co(1)–O(2)	2.074(7)	2x	Co(1)–O(1)	2.094(5)	2x
Co(1)–N(1)	2.153(2)	2x	C(1)–C(1A)	1.582(5)	
O(1)–C(1)	1.293(12)		O(2)–C(1B)	1.206(13)	
N(1)–C(2)	1.317(3)		C(2)–C(3)	1.381(3)	
C(3)–C(4)	1.369(3)		C(4)–C(4E)	1.489(5)	
O(2)–Co(1)–O(2A)	82.4(3)		O(2)–Co(1)–O(1)	178.5(3)	
O(2A)–Co(1)–O(1)	99.09(8)	2x	O(2A)–Co(1)–O(1A)	178.5(3)	
O(1)–Co(1)–O(1A)	79.4(3)		O(2)–Co(1)–N(1A)	90.0	2x
O(1)–Co(1)–N(1A)	90.0	2x	O(2)–Co(1)–N(1)	90.0	2x
O(1)–Co(1)–N(1)	90.0	2x	N(1A)–Co(1)–N(1)	180.0(3)	
C(1)–O(1)–Co(1)	115.3(5)		C(1B)–O(2)–Co(1)	110.3(5)	
C(2)–N(1)–Co(1)	122.04(12)	2x	O(2D)–C(1)–O(1)	126.5(2)	
O(2D)–C(1)–C(1A)	118.5(5)		O(1)–C(1)–C(1A)	115.0(4)	
C(2C)–N(1)–C(2)	115.9(2)		N(1)–C(2)–C(3)	123.9(2)	
C(4)–C(3)–C(2)	120.1(2)		C(3)–C(4)–C(3C)	116.1(3)	
C(3)–C(4)–C(4E)	121.97(13)	2x			

Symmetry transformations used to generate equivalent atoms: A $-x+1, -y, z$; B $-x+1, -y, z-1$; C $-x+1, y, z$; D $-x+1, -y, z+1$; E $-x+1, -y+1, z$.

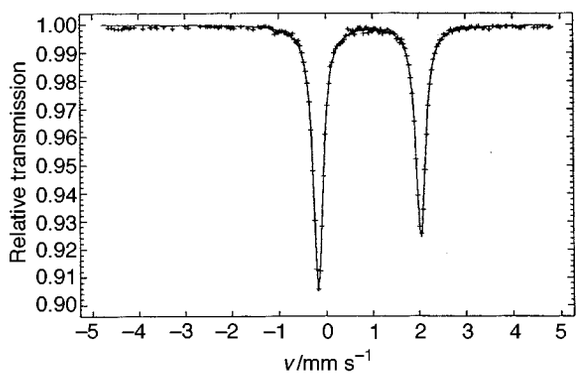

Fig. 5 Mössbauer spectrum of compound **1** at 298 K.

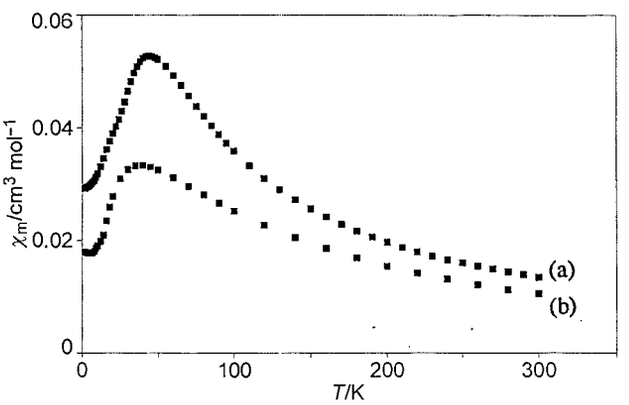

Fig. 6 Temperature dependent molar magnetic susceptibilities for compounds **1** (a) and **2** (b).

The higher value of μ_{eff} is attributed to the orbital contribution of the high spin iron(II) center. The maximum around 44 K in Fig. 6(a) suggests the presence of an antiferromagnetic coupling, which is confirmed by a negative Weiss constant (−16.0 K) determined in the temperature range 300–100 K using the equation $\chi_m = C/(T - \theta)$.

The magnetic behavior of compound **2** is quite similar to that of **1** [Fig. 6(b)]. At 300 K the effective magnetic moment per Co (5.02 μ_B) is much greater than the spin-only value (3.87 μ_B) expected for a high spin ($S = 3/2$) center, which originates from an orbital contribution of Co^{II}. The maximum around 40 K in Fig. 6(b) indicates that an antiferromagnetic interaction is propagated.

The layered structures of compounds **1** and **2** contain metal(II) oxalate chains linked by 4,4′-bipyridine molecules. It is well known that an efficient antiferromagnetic exchange can be transmitted through the oxalate bridge.[24] The magnetic interaction through the 4,4′-bipyridine bridge, however, is usually very weak considering the long M···M distances of *ca.* 11.5 Å. This interaction could be further reduced because of the twist of the two pyridine rings as in the case of **1**. Therefore, it is reasonable to describe the magnetic behaviors of both compounds based on a chain model. The M···M separations through the oxalate ligand are 5.397–5.431 Å in **1** and 5.403 Å in **2**. The three interaction parameters in **1** may be assumed to be very close to each other. The susceptibility data were then analyzed by using an expression for the magnetic susceptibility of a uniform chain of classical spins derived by Fisher, with the classical spins scaled to a real quantum spin $S = 2$ for **1** and 3/2 for **2**.[24,32] The equation, however, does not fit the experimental data well, especially at low temperatures (<44 K). The inclusion of an interchain exchange based on the molecular field approximation does not improve the theoretical fitting distinctly. The bad fits for both compounds may be explained by the fact that Fisher's equation does not take into account the effects of the zero-field splitting and/or spin–orbital coupling which could be significant for iron(II) and cobalt(II) ions.

In conclusion, this paper describes two new layered compounds $[Fe_3(C_2O_4)_3(4,4'\text{-bpy})_4]$ and $[Co(C_2O_4)(4,4'\text{-bpy})]$, containing both 4,4′-bpy and oxalate bridging ligands. The magnetic properties indicate antiferromagnetic exchanges in both compounds which should be mediated mainly through the oxalate bridges. Further work is in progress, using mixed bridging ligands, to build up novel polymeric, microporous co-ordination networks with tunable pore size and interesting properties.

Acknowledgements

This work is supported by the National Natural Science Foundation, Natural Science Foundation of Jiangsu Province of China, the Education Commission of China and Malaysian Government research grant R&D (No. 190-9609-2801). We are grateful to Professor S.-L. Wang and Ms F.-L. Liao at Tsing Hua University for X-ray intensity data collection for compound **1**, to Dr Z. Yu at Nanjing University for assistance in collecting and fitting the Mössbauer data, and to Professor G. X. Wang at Nanjing University for stimulating discussions.

References

1 H. Tamaki, Z. J. Zhong, N. Matsumoto, S. Kida, N. Koikawa, Y. Achiwa, Y. Hashimoto and H. Okawa, *J. Am. Chem. Soc.*, 1992, **114**, 6974.

2 L. O. Atovmyran, G. V. Shilov, R. N. Lyubovskaya, E. I. Zhilyacva, N. S. Ovanesyan, S. I. Pirumova and I. G. Gusakovskaya, *JETP Lett.*, 1993, **58**, 766.
3 S. Decurtins, H. W. Schmalle, P. Schneuwly and H. R. Oswald, *Inorg. Chem.*, 1993, **32**, 1888.
4 S. Decurtins, H. W. Schmalle, H. R. Oswald, A. Linden, J. Ensling, P. Gutlich and A. Hauser, *Inorg. Chim. Acta*, 1994, **216**, 65.
5 S. Decurtins, H. W. Schmalle, P. Schneuwly, J. Ensling and P. Gutlich, *J. Am. Chem. Soc.*, 1994, **116**, 9521.
6 C. Mathonière, C. J. Nuttall, S. G. Carling and P. Day, *Inorg. Chem.*, 1996, **35**, 1201.
7 M. Clemente-León, E. Coronado, J.-R. Galán-Mascarós and C. J. Gómez-García, *Chem. Commun.*, 1997, 1727.
8 J. Larionova, B. Mombelli, J. Sanchiz and O. Kahn, *Inorg. Chem.*, 1998, **37**, 679.
9 M. Hernández-Molina, F. Lloret, C. Ruiz-Pérez and M. Julve, *Inorg. Chem.*, 1998, **37**, 4131.
10 G. De Munno, M. Julve, F. Nicolo, F. Lloret, J. Faus, R. Ruiz and E. Sinn, *Angew. Chem.*, *Int. Ed. Engl.*, 1993, **32**, 613.
11 G. De Munno, R. Ruiz, F. Lloret, J. Faus, R. Sessoli and M. Julve, *Inorg. Chem.*, 1995, **34**, 408.
12 S. Decurtins, H. W. Schmalle, P. Schneuwly, L.-M. Zheng, J. Ensling and A. Hauser, *Inorg. Chem.*, 1995, **34**, 5501.
13 S. Kitagawa, T. Okubo, S. Kawata, M. Kondo, M. Katada and H. Kobayashi, *Inorg. Chem.*, 1995, **34**, 4790.
14 J. Lu, C. Yu, T. Niu, T. Paliwala, G. Crisci, F. Somosa and A. J. Jacobson, *Inorg. Chem.*, 1998, **37**, 4637.
15 M. Fujita, Y. J. Kwon, S. Washizu and K. Ogura, *J. Am. Chem. Soc.*, 1994, **116**, 1151.
16 M. Kondo, T. Yoshitomi, K. Seki, H. Matsuzaka and S. Kitagawa, *Angew. Chem.*, *Int. Ed. Engl.*, 1997, **36**, 1725.
17 O. M. Yaghi, H. Li and T. L. Groy, *Inorg. Chem.*, 1997, **36**, 4292.
18 O. M. Yaghi and H. Li, *J. Am. Chem. Soc.*, 1995, **117**, 10401.
19 O. M. Yaghi and H. Li, *J. Am. Chem. Soc.*, 1996, **118**, 295.
20 A. J. Blake, S. J. Hill, P. Hubberstey and W.-S. Li, *J. Chem. Soc.*, *Dalton Trans.*, 1997, 913.
21 S. Subramanian and M. J. Zaworotko, *Angew. Chem.*, *Int. Ed. Engl.*, 1995, **34**, 2127.
22 M. L. Tong, B. H. Ye, J. W. Cai, X.-M. Chen and S. W. Ng, *Inorg. Chem.*, 1998, **37**, 2645.
23 N. Masciocchi, P. Cairati, L. Carlucci, G. Mezza, G. Ciani and A. Sironi, *J. Chem. Soc.*, *Dalton Trans.*, 1996, 2739.
24 O. Kahn, *Molecular Magnetism*, VCH, New York, 1993.
25 *SHELXTL Version 5.0 Reference Manual*, Siemens Analytical X-Ray Systems, Inc., Madison, WI, 1996.
26 J. T. Wrobleski and D. B. Brown, *Inorg. Chem.*, 1979, **18**, 2738.
27 J. G. Contreras and C. J. Diz, *J. Coord. Chem.*, 1987, **16**, 245.
28 H.-K. Fun, S. S. S. Raj, X. Fang, L.-M. Zheng and X.-Q. Xin, *Acta Crystallogr.*, 1999, in the press.
29 L.-M. Zheng, X. Chen, S. Gao, K. Chinnakali and H.-K. Fun, submitted for publication.
30 F. D. Rochon, R. Melanson and M. Andruh, *Inorg. Chem.*, 1996, **35**, 6086.
31 M. Molinier, D. J. Price, P. T. Wood and A. K. Powell, *J. Chem. Soc.*, *Dalton Trans.*, 1997, 4061.
32 M. E. Fisher, *Am. J. Phys.*, 1964, **32**, 343.

Paper 8/09738K